Published in final edited form as:
Nat Cell Biol. 2017 May ; 19(5): 568–577. doi:10.1038/ncb3516.

Long-term, hormone-responsive organoid cultures of human endometrium in a chemically-defined medium

Margherita Y. Turco[1,11,*], **Lucy Gardner**[1,11], **Jasmine Hughes**[2], **Tereza Cindrova-Davies**[3,11], **Maria J. Gomez**[1], **Lydia Farrell**[1,11], **Michael Hollinshead**[1], **Steven G.E. Marsh**[4], **Jan J. Brosens**[5], **Hilary O. Critchley**[6], **Benjamin D. Simons**[7,8], **Myriam Hemberger**[9,11], **Bon-Kyoung Koo**[8,10], **Ashley Moffett**[1,11,12], and **Graham J. Burton**[3,11,12,*]

[1]Department of Pathology, University of Cambridge, UK

[2]Department of Clinical Medicine, Addenbrooke's Hospital, University of Cambridge, UK

[3]Department of Physiology, Development and Neuroscience, University of Cambridge, UK

[4]Anthony Nolan Research Institute, Royal Free Hospital, London, UK

[5]Division of Reproductive Health, Clinical Science Research Laboratories, Warwick Medical School, University of Warwick, Coventry, UK

[6]MRC Centre for Reproductive Health, University of Edinburgh, UK

[7]Gurdon Institute and Department of Physics, University of Cambridge, UK

[8]Wellcome Trust - Medical Research Council Stem Cell Institute, University of Cambridge, UK

[9]Epigenetics Programme, The Babraham Institute, Babraham Research Campus, Cambridge, UK

[10]Department of Genetics, University of Cambridge, UK

[11]Centre for Trophoblast Research, University of Cambridge, UK

Abstract

In humans, the endometrium, the uterine mucosal lining, undergoes dynamic changes throughout the menstrual cycle and pregnancy. Despite the importance of the endometrium as the site of implantation and nutritional support for the conceptus, there are no long-term culture systems that recapitulate endometrial function *in vitro*. We adapted conditions used to establish human adult

[*]Correspondence: G.J. Burton (gjb2@cam.ac.uk) and M.Y. Turco (myt25@cam.ac.uk).
[12]Co-last authors

Author Contributions

M.Y.T. and L.G. designed, carried out all experiments and data analyses; J.H. and T.C-D. assisted with experiments and data analyses; M.J.G. performed microarray analysis; M.H. performed EM analysis and assisted with confocal analysis; J.J.B. and H.C. provided endometrial specimens and input for the manuscript; L.F. and S.G.E.M. assisted with experiments; A.M and B.K.K. assisted with experimental design, analyses of results and preparation of manuscript; B.J.S and M.H. assisted with analyses of results and preparation of manuscript; M.Y.T., A.M. and G.J.B. wrote the manuscript.

Data availability. Microarray data that support the findings of this study have been deposited in the Gene Expression Omnibus (GEO) under accession codes GSE83281 (Figure 2 and Supplementary Figure 2) and GSE94723 (Figure 3). Source data for Figures 1b, 1e, 3e, 3g and Supplementary figure 6b have been provided as Supplementary Table 5. All other data supporting the findings of this study are available from the corresponding authors upon reasonable request.

Europe PMC Funders Author Manuscripts

stem cell-derived organoid cultures to generate 3D cultures of normal and decidualised human endometrium. These organoids expand long-term, are genetically stable and differentiate following treatment with reproductive hormones. Single cells from both endometrium and decidua can generate a fully functional organoid. Transcript analysis confirmed great similarity between organoids and the primary tissue of origin. On exposure to pregnancy signals, endometrial organoids develop characteristics of early pregnancy. We also derived organoids from malignant endometrium, and so provide a foundation to study common diseases, such as endometriosis and endometrial cancer, as well as the physiology of early gestation.

Throughout adult reproductive life, the functional layer of the human endometrium undergoes a monthly cycle of regeneration, differentiation and shedding under the control of the hypothalamic-pituitary-ovarian (HPO) axis. The mucosa contains simple glands lined by secretory columnar epithelium, separated by intervening stroma. During the estrogen-dominated proliferative phase that follows menstruation, the mucosa regrows and then differentiates during the progesterone-dominated secretory phase. Implantation occurs ~7 days post-ovulation onto the ciliated luminal epithelium and stimulates transformation into the gestational endometrium, the true decidua of pregnancy, that provides a microenvironment essential for placentation. Up to ~10 weeks gestation, uterine glands provide histotrophic nutrition for the conceptus before the definitive hemochorial placenta is established1, 2. Animal models in mice and ruminants where glandular function is suppressed are unable to support implantation and pregnancy3, 4. Such models have revealed the molecular interactions involved between the trophectoderm and the uterine surface and the key cytokines secreted by the glands, such as leukemia inhibitory factor5. However, the composition of the secretions, and the gland/conceptus signalling dialogue during human placentation are unknown due to their inaccessibility *in vivo* and the absence of *in vitro* models. Suboptimal glandular development and/or functions may result in human pregnancy failure or predispose to complications of later pregnancy, such as growth restriction6. Thus, model systems to study these essential processes of human early pregnancy would have many biological and clinical applications.

Although stem/progenitor cells within the stromal compartment of the endometrium have been identified, suitable markers for glandular progenitors are unknown7. In mice, stem cells are probably present at the base of the glands8; similarly in primates, cells in the basal layer, that is not shed during menstruation, can generate both glandular and luminal epithelia9, 10. In humans, putative endometrial stem cells are the rare SSEA-1+, SOX9+ population with clonogenic ability11, 12 but these are not fully characterised and it is unknown how they maintain uterine glands. Previous culture systems of human endometrial glandular cells, including 3D cultures, do not fully recapitulate glandular features *in vivo*, and are not long-term or chemically defined13, 14. Establishing defined endometrial organoid cultures will offer possibilities for studying events during implantation and early pregnancy *in vitro* as human blastocysts can be cultured past the implantation phase of development15, 16.

Organoids are self-organising, genetically stable, 3D culture systems containing both progenitor/stem and differentiated cells that resemble the tissue of origin. Human organoids have been derived from tissue-resident adult epithelial stem cells from gut, liver, pancreas,

prostate and fallopian tube17–21. We have now generated long-term, chemically-defined 3D glandular organoid cultures from non-pregnant endometrium and decidua. The organoids recapitulate features of uterine glands *in vivo*; the ability to respond to hormonal signals, secrete components of uterine 'milk' and differentiate into ciliated luminal epithelial cells. Human endometrial organoids can be used to answer questions about uterine/placental cross-talk during placentation, and will provide a system for studying the pathogenesis and treatment of common conditions affecting women, such as endometriosis and endometrial cancer.

Results

Long-term genetically-stable 3D organoid cultures can be established from human non-pregnant endometrium and decidua

To generate endometrial organoids, we used tissue isolates enriched for epithelial cells, and allowed these to self-organise within Matrigel droplets with the basal medium that supports development of other human tissue organoids, containing EGF, Noggin and R-spondin-1 (ENR) (Fig. 1a). Because the signalling pathways maintaining endometrial gland stem/progenitor cells are unknown, we tested factors secreted by surrounding stromal cells, FGF10 and HGF22–25. Nicotinamide and the Alk3/4/5 inhibitor, A83-01, that blocks the TGFβ pathway were added as they are crucial in the establishment and/or long-term culture of other human organoid systems18, 20, 26. Decidual samples were initially used to optimise the culture conditions as they yield high cell numbers. Glandular cells were cultured for 7 days and passaged at 1:3. Organoid numbers were counted after another 7 days (Fig. 1b,c). A83-01, FGF10 and HGF with EGF, Noggin, R-spondin-1 and nicotinamide, expansion medium (ExM), gave the highest yield of cells (Fig. 1c, C8).

Organoid cultures were established in ExM within 1-2 passages (Fig. 1d). To assess the requirement for each culture component, 5000 cells were plated from established cultures (grown for >4 passages) in the absence of each factor, and the number of spheroids present after one week counted. Withdrawal of nicotinamide had the strongest effect, whilst the lack of Noggin, Rspondin-1, A83-01, EGF and HGF resulted in reduced numbers and/or smaller organoids (Fig. 1e, Supplementary Fig. 1a). FGF10 was maintained in the medium even though it had no effect on size or numbers of organoids (Fig. 1e), because it was important initially in establishing cultures and provides a physiological environment (Fig. 1b). ENR, A83-01 and nicotinamide will maintain established cultures, but were not tested in differentiation experiments and long-term culture (Supplementary Fig. 1b). Organoid cultures were robustly established from decidual samples in ExM from 25/26 donors (derivation efficiency of 96%). Organoids were then successfully generated from non-pregnant secretory endometrium with 100% derivation efficiency (11/11) (Fig. 1f). Proliferative phase endometrium is infrequently sampled, but we did generate organoids from this phase (n=3) and from atrophic endometrium (n=1), demonstrating that our culture conditions can be used for tissue throughout the menstrual cycle, as well as pregnant and post-menopausal endometrium (Fig. 1f). The origin and characterization of established organoid cultures used for this study are summarized in Supplementary Table 1.

The established organoids can be expanded at passage ratios of 1:2 or 1:3 every 7-10 days for >6 months (reaching more than a 10^6-fold increase in the number of organoids). Markers of glandular epithelium (MUC1, E-CADHERIN, CK7 and EPCAM) are strongly expressed by the organoids (Fig. 1g,h,i). EPCAM and LAMININ are present at the baso-lateral membrane, showing epithelial polarity is intact (Fig. 1i). EdU pulse-labelling shows ~30% of cells are actively replicating (Fig. 1i). The organoids form cystic structures lined by columnar epithelium with secretions visible in the lumen. Electron microscopy reveals a microvillous, pseudostratified columnar epithelium supported by amorphous basement membrane material with basally-located nuclei (Fig. 1j). The cytoplasm contains plentiful rough endoplasmic reticulum and Golgi bodies, numerous secretory vesicles, with evidence of secretory activity from the apical surface (Fig. 1k, arrowheads). A major component of endometrial glandular secretions, glycogen, was visualized by vivid PAS staining (Fig. 1l). Thus, the appearances are highly similar to endometrial glands *in vivo*27.

Next, the chromosomal stability of our endometrial organoids was checked by Comparative Genomic Hybridization (CGH) array. Genomic DNAs were compared between the patient and established organoid cultures at early passage (p) (2-4p) and between early and late cultures (8-15p) (Supplementary Fig. 1d-f). No significant DNA copy number abnormalities were identified during derivation or after continuous passaging for up to 5 months. These organoids can be frozen, thawed and regrown, allowing bio-banking of human endometrial cultures.

Established human endometrial gland organoids recapitulate molecular signature of glands *in vivo*

To assess the similarity between organoids and the tissue of origin, we analysed the global gene expression profiles from established organoid lines (n=7), initial glandular digests, and cultured stromal cells from the same biopsy. Staining for MUC1 (glands) and VIMENTIN (stroma) confirmed enrichment of glands in our isolates and the purity of stromal cultures (Supplementary Fig. 2a-d). Hierarchical clustering analysis based on 15,475 probes (sd/mean >0.1) shows that the organoid cultures cluster more closely to glands than to stroma, confirming their glandular epithelial nature (Fig. 2a).

To define an endometrial glandular genetic signature, we compared glands and organoids to stroma. 287 genes were commonly upregulated in organoids and glands compared to stroma with a fold change of ≥1.5 ($p \leq 0.01$) (Fig. 2b). Gene ontology (GO) analysis shows enrichment for ‘epithelial identity’ and ‘glandular function’ (Fig. 2c,d). Markers of epithelial cells (*CDH1, CLDN10* and *EPCAM),* mucosal secretory cells (*PAX8 and MUC1*) and of uterine glandular products were all present (*PAEP*, *KLK11* and *MUC20*) (Fig. 2e). Murine genes involved in endometrial glandular development and function (*FoxA2, Sox17* and *Klf5)* also emerged4, 28–31. Using immunohistochemistry, we verified nuclear presence of FOXA2, SOX17 and PAX8 in all organoids and endometrial glandular cells throughout the cycle (Fig. 2f). Markers (*PROM1*, *AXIN2* and *LRIG1*) common to other epithelial progenitor cells32, 33 were found (Fig. 2e), but in endometrium *LRIG1* transcripts are present in glands and luminal epithelium throughout the cycle and so their significance is uncertain (Fig. 2g, Supplementary Fig. 3a). Analysis of expression of other putative

endometrial stem cell markers, *AXIN2* and SSEA1 was inconclusive11. Although *AXIN2* transcripts were found in glands *in vivo*, lack of a reliable antibody prevented further analysis (Supplementary Fig.3b). Only a few cells were SSEA-1+ in organoids, analysed by immunohistochemistry and flow cytometry (2-3%) and, after sorting SSEA-1+/- cells, organoids emerged from the SSEA-1-negative fraction (Supplementary Fig. 3c, d). Overall the gene signature of decidual organoids (n=6) is also very similar to non-pregnant endometrium (Supplementary Fig. 4a), with immunostaining of FOXA2, SOX17 and PAX8 and expression of *LRIG1* uniformly similar to *ex vivo* decidual glands (Supplementary Fig. 4b,c).

Apart from shared gene sets between glands and organoids, there are also genes only expressed in glands (421/652) or organoids (286/484) (Supplementary Fig. 5). GO terms for glands describe stromal interactions (integrin binding and extracellular matrix structural constituents), all absent *in vitro.* For organoids, *in vitro* proliferation, (cell division and mitotic nuclear division) dominated. Thus, differential gene expression between gland samples and organoids reflects their contrasting microenvironments.

A converse analysis to define a stromal cell signature (Supplementary Fig. 2e) revealed minimal contamination from endothelial cells (*CD31* or *CD34*) or leukocytes (*CD45*). GO analysis showed ‘biological processes’ typical of fibroblasts and ‘molecular functions’ (Supplementary Fig. 2f, g). Gene sets were enriched for stromal cell markers (*THY1*, *NT5E* and *IFITM1*)34, 35, extracellular matrix proteins (*COL8A1, COL12A1*, *COL13A1* and *LAMA1*), and metalloproteinases (*MMP11, MMP2, MMP12, MMP27, MMP3*, *TIMP2* and *CTGF*) (Supplementary Fig. 2e). Genes encoding for components of WNT (*WNT2, WNT5A, RSPO3*), BMP (*BMP2, GREM1*) and MAPK (*FGF2*) signalling pathways also emerged, pathways already identified from our culture conditions.

Human endometrial gland organoids respond to sex hormones

Unlike other mucosal epithelia, the endometrium responds dramatically to ovarian hormones, estrogen (E2) and progesterone (P4), which regulate cyclical proliferation and differentiation of endometrial glands with concomitant dynamic temporal and spatial expression of their receptors, ERα and PR (Fig. 3a)36–38. Following menstruation, glands increase expression of ERα in response to rising E2 levels (proliferative phase). After ovulation, ERα expression declines in the early secretory phase whereas PR is maintained until mid-secretory (LH+7), after which both ERα and PR expression disappears37.

To mimic the response of the organoid cultures to hormones, we exposed organoids to E2 followed by P4 (Fig. 3b). Under ExM conditions most cells show weak expression of ERα ($ERα^{low}$) with some $ERα^{high}$ (Fig. 3c, arrowheads) and $ERα^{negative}$ cells (Fig. 3c, arrows) present. Although most organoids are $PR^{negative}$, a few cells are PR^{high}; on serial sections these are also $ERα^{high}$. After exposure to E2 and P4, high expression of both ERα and PR is seen in most organoids similar to the situation *in vivo* (Fig. 3c). Organoid cultures derived from decidua showed similar responses (Supplementary Figure 6a).

We performed a microarray analysis of organoids in ExM, E2 alone or E2 and P4. Known genes upregulated by E2 and P4 in the mid-secretory phase *17βHSD2, PAEP, SPP1, LIF,*

IGFBP4, IGFBP5 and *CYCLIN A1* were all upregulated in hormonally-treated organoids (Fig. 3d)39–42. This was confirmed for several genes using qRT-PCR (Fig. 3e) and at the protein level for PAEP and SPP1 (Fig. 3 f,g). We also confirmed that the addition of cyclic adenosine monophosphate (cAMP) to the differentiation medium, a component used typically in decidualization protocols, enhances the expression of differentiation markers shown by increased expression of *PAEP* and *SPP1* (Supplementary Fig. 6b)43.

Other hormonally-regulated endometrial genes emerged, including *OLFM4*, an intestinal stem cell marker44. In ExM, organoid cells were OLFM4-negative but a subset became OLFM4-positive after E2 treatment, similar to the proliferative phase *in vivo* (Fig. 3h, arrows). *Collagen 1A2 (COL1A2), chromogranin A (CHGA)* and *OVOL2* were also upregulated, whilst *HES1* and *SOX9* were downregulated. In summary, the phenotypic response of glandular endometrial organoids to ovarian sex hormones is characteristic of the early-mid secretory phase.

Signals from decidualised stroma and the placenta can further stimulate differentiation of human endometrial gland organoids

If implantation occurs, the endometrium forms the true decidua of pregnancy in response to P4; decidualized stromal cells characteristically secrete Prolactin (PRL) 45 (Fig. 4a). Both PRL and signals from the conceptus are likely to stimulate uterine gland activity in early pregnancy (Fig. 4a)46, 47. To mimic pregnancy, we added placental hormones (Chorionic Gonadotropin, hCG and human Placental Lactogen, hPL) in combinations with PRL to ExM containing E2+P4+cAMP, referred to as Differentiation Medium (DM) (Fig. 4b).

The three hormones together stimulate maximal production of PAEP and a hypersecretory morphology characteristic of decidual glands *in vivo* (Fig. 4c). PRL has an additional effect by stimulating the formation of ciliated cells (identified by acetylated α-tubulin) (Fig. 4d). Similar findings were obtained using conditioned media from stromal cells decidualized *in vitro* for 10 days (Supplementary Figure 6c). As ciliated cells are only present *in vivo* in the uterine luminal epithelium and in superficial glands, the organoids are undergoing both glandular and luminal differentiation.

SOX9, a marker of progenitor cells, is expressed in the base of endometrial glands *in vivo* and at high levels in the organoids11, 48, 49 but is absent from decidual glands *in vivo.* Organoids cultured with both ovarian and pregnancy hormones undergo differentiation as SOX9 was downregulated (Fig. 4e). Thus, appropriate hormonal stimulation induces organoids to acquire a decidual-like phenotype characteristic of early pregnancy.

Human endometrial organoids have clonogenic ability and are bipotent

To assess for stem cell activity, we measured clonogenic ability by plating single cells from established organoid cultures by limiting dilution; drops containing single cells were marked and followed by time-lapse photography. Some cells formed an entire organoid over 7-14 days; the rest either did not divide or formed small dying spheroids (Fig. 5a). The organoid-forming efficiency of these cells, was 2-4% with 100 cells/drop and ~10-fold lower with 10 cells/drop (Supplementary Table 2). Single organoids can be expanded into clonal cultures and we now have grown 12 clonal lines from 5 independently-derived organoids (Fig. 5b). A

single cell has bi-potent ability as it could generate the two main endometrial cell types: secretory (PAEP+) and ciliated (acetylated-α-tubulin+) cells (Fig. 5c). Formation of cilia was confirmed by EM (Fig. 5d).

Organoid cultures can be derived from endometrial cancer

Endometrial cancer is the commonest gynecological tumour. Organoids were derived from samples of tumours and the normal adjacent endometrium from post-menopausal women (Fig. 6). The morphology of the organoids resembles the primary tumour (FIGO Grade I Endometrioid Carcinoma) showing pleomorphic cells with hyperchromatic nuclei and disorganised epithelium. In places breaching of the basement membrane is obvious, and isolated cells are seen in the surrounding Matrigel. The organoids are positive for glandular markers such as MUC1 and SOX17, confirming their glandular origin.

Discussion

Here, we describe a robust chemically-defined method for establishing genetically stable endometrial organoids from human non-pregnant endometrium and decidua that can be cultured long-term and recapitulate the molecular signature of endometrial glands *in vivo.* Several murine genes important for glandular development and function (*Foxa2*, *Klf5* and *Sox17*) are also expressed. The organoids functionally respond to sex hormones, E2 and P4, and when further stimulated with pregnancy (hCG, hPL) and stromal cell (PRL) signals, acquire characteristics of gestational endometrium, synthesising abundant PAEP (glycodelin) and SPP1 (osteopontin). PAEP and SPP1, components of glandular secretions, ‘uterine milk’, provide histotrophic nutrition to trophoblast before the hemochorial placenta is established.

Clonal organoid cultures generated from a single cell contain cells with extensive proliferative capacity, and both ciliated and secretory cells. Their gene signature includes markers of epithelial stem cells, *LRIG1, PROM1, AXIN2* and *SOX9*. Because we could generate SOX9-expressing organoids from non-proliferative, SOX9-, differentiated secretory phase endometrium and decidua, the few SOX9+ cells present mainly in the basal layer might expand11. Alternatively, plasticity of endometrial cells allows SOX9-negative differentiated cells to self-renew and reacquire SOX9 expression in our cultures. A similar reversion occurs in the liver, where non-Lgr5+ cells reacquire Lgr5 stem cell marker expression upon tissue injury50.

Although organoids have been established from human fallopian tube with differentiation into both ciliated and secretory cells, neither the dramatic cyclical changes in response to E2 and P4, nor the process of decidualization induced by pregnancy occurs in the fallopian tube, a mucosal surface contiguous to endometrium21. Furthermore, the crucial site of embryo attachment is the luminal surface of the endometrium.

Endometrial organoids can be maintained and expanded in ExM, recapitulating pathways essential for culturing organoids from other organs - the FGF-MAPK, WNT-Rspondin, BMP-Noggin and TGFβ signalling pathways51. The contribution of endometrial stromal cells to these signalling pathways is revealed from our microarray analysis showing stromal

transcripts encoding Rspondin-1 and FGF2. Further refinement of the method to replace Matrigel with a chemically-defined extracellular matrix would enhance the model in future52. The identity of the endometrial epithelial stem cells remains unknown although their presence is revealed by the long-term expansion and clonogenic activity of organoids, and we have defined the essential niche components for their maintenance.

We also recapitulate the glandular cyclical changes during the menstrual cycle triggered by sequential secretion of ovarian hormones, E2 and P4. Endometrial organoids acquire a differentiated phenotype characteristic of the mid-secretory phase, with upregulation of several genes (*17βHSD2*, *SPP1*, *LIF*) expressed at this time. Other genes, such as *OLFM4*, that may play key roles in regulating gland cell proliferation and function during the cycle were also identified.

Besides the direct effect E2 and P4 have on the glands, they also exert a paracrine effect via the stromal cells. Decidualized stroma secretes a wide range of proteins, including PRL whose function is unknown. Unlike the pituitary, decidual PRL is driven from an alternative promoter, derived from transposable elements (MER20)53. Our finding that addition of PRL induces ciliated cells suggests it may influence differentiation and function of the glands during early pregnancy.

The glands of gestational endometrium continue to differentiate and display a hypersecretory appearance with abundant PAEP production54, 55. In our organoid system, addition of trophoblast hormones (hCG and hPL) resulted in a similar appearance. This culture system will therefore allow further investigation of the essential (but understudied) period of histotrophic nutrition in the first trimester of pregnancy before the hemochorial placenta is established. Additionally, we were able to derive organoids from endometrial adenocarcinomas. These common tumours in post-menopausal women are associated with increased exposure to estrogen that is a feature of obesity, nulliparity, treatment with tamoxifen and late menopause56. These can be used in the future to build a biobank to screen drugs and investigate the mutational changes, as has been done for colon cancers57.

In summary, we describe a method for reliable chemically-defined, long-term culture of endometrial glands from non-pregnant endometrium and decidua that closely recapitulates the molecular and functional characteristics of their cells of origin. The organoid cultures can be frozen down without loss of their proliferative ability upon thawing, allowing the possibility to build up patient-specific bio-banks. This method will be an invaluable research tool to study new therapies for common pathologies of the endometrium, such as endometriosis and endometrial cancer, as well as investigating problems of implantation and the secretion of uterine histotroph during early pregnancy.

Methods

Patient samples

All tissue samples used for this study were obtained with written informed consent from all participants in accordance with the guidelines in The Declaration of Helsinki 2000 from multiple centres:

(i) Decidual samples were obtained from elective terminations of normal pregnancies at Addenbrooke's Hospital between 8 and 12 weeks gestation under ethical approval from the Cambridge Local Research Ethics Committee (04/Q0108/23).

(ii) Secretory phase (6 and 10 d after pre-ovulatory luteinizing hormone surge) endometrial samples were obtained from subjects recruited from the Implantation Clinic at University Hospitals Coventry and Warwickshire National Health Service Trust with ethical approval from NHS National Research Ethics – Hammersmith and Queen Charlotte's & Chelsea Research Ethics Committee (1997/5065). Endometrial biopsies were obtained using a Wallach EndocellTM sampler, starting from the uterine fundus and moving downward to the internal cervical ostium. None of the subjects were on hormonal treatments for at least 3 months prior to the procedure.

(iii) Proliferative and secretory endometrial samples were obtained from Addenbrooke's Hospital under ethical approval from the East of England - Cambridge South Research Ethics Committee (08/H0305/40).

(iv) Endometrial carcinoma samples were obtained from Addenbrooke's Hospital Tissue Bank.

(v) Proliferative and secretory human endometrial tissue sections for immunohistochemistry and *in situ* hybridisation studies were available with research ethical committee approval (Lothian Research Ethics Committee: 10/S1402/59; 16/ES0007). Endometrial tissues were staged based on standard histological criteria and circulating oestradiol and progesterone levels at the time of collection and no exogenous hormone exposure.

Isolation of glands, derivation and culture of organoids from human uterine tissue samples

Endometrial/decidual/carcinoma tissues were chopped using scalpels into approximately 0.5 mm^3 cubes and enzymatically digested in 20-30 mL 1.25U/mL Dispase II (Sigma, D4693)/0.4mg/mL collagenase V (Sigma, C-9263) solution in RPMI 1640 medium (ThermoFisher Scientific, 21875-034)/10% FCS (Biosera, FB-1001) with gentle shaking at 37°C for 30-60 min. The supernatant was passed through one or more 100 μm cell sieves (Corning, 431752) and the sieve washed several times with medium. The flow-through was collected for stromal cell culture in Advanced DMEM/F12 (ThermoFisher Scientific, 12634010) +10%FBS+pen/strep (Sigma, P0781) +L-glutamine (Sigma, 25030-024) for several days and subsequent analysis. The sieves were inverted over a petri dish and retained glandular elements were backwashed from the sieve membranes, pelleted by centrifugation and resuspended in ice cold Matrigel (Corning, 536231) at a ratio of 1:20 (vol:vol). 20 μL drops of Matrigel-cell suspension were plated into 48-well plate (Costar, 3548), allowed to set at 37°C and overlaid with 250 μL organoid Expansion Medium (ExM). See Supplementary Table 3 for ExM composition. The medium was changed every 2-3 d. Cultures were passaged by manual pipetting every 7-10 d. For freezing organoids, Matrigel was removed using Cell Recovery Solution (Corning, 354253) and organoids were resuspended in

Recovery cell culture freezing medium (ThermoFisher Scientific, 12648-010). A step-by-step protocol of the derivation and maintenance of human endometrial organoid cultures can be found at Nature Protocol Exchange59.

Organoid formation efficiency assays

Organoids were removed of Matrigel using Cell Recovery Solution and pipetted several hundred times before trypsinizing with TrypLE Express (Invitrogen, 12604-013). Cells were washed in medium and passed through a 40 μm cell strainer (Corning, 352340) to ensure single cell suspension. Cells were diluted in trypan blue to exclude dead cells and counted using haematocytometer. For the growth factor requirement experiment (Fig.1e), 5000 cells were plated per 20 μL Matrigel drop into 48 well plate, per culture condition in triplicate. The number of organoids formed after 7 d were scored. For organoid formation efficiency assay (Supplementary Table 2), 100 cells were plated into 5 μL Matrigel drops into 96-well plate (ThermoFisher Scientific, 167008) and overlayed with 100 μL medium. The number of organoids were scored after 10 d.

Single cell organoid formation timecourse

Organoids were processed in the same way as for organoid formation efficiency assay. Cells were then plated using limiting dilution assay technique to have approximately 1 cell per 2.5 μL Matrigel drop. The drops were plated onto gridded 35 mm ibidi glass bottom dishes (Thermo Scientific, 81148) and overlayed with 1.2 mL of ExM. ExM was supplemented with 10 μM Y-27632 (Merck, 688000) for first 3 d of culture. Drops were screened and the relative positions of the drops containing one cell were stored using the Axiovision image software V4.8 and cells were imaged in phase contrast every 2 d using the Zeiss Axiovert Z1 microscope and Axio Observer software.

Differentiation of endometrial organoids

For hormonal stimulation of organoids with β-estradiol (E2, Sigma E4389), Progesterone (P4, Sigma P7556) and 8-Bromoadenosine 3', 5'-cyclic monophosphate (cAMP, Sigma B7880), organoids were passaged routinely and after 4 d of growth in ExM, they were primed with 10 nM E2. After 48 h, medium was replaced with the following conditions: i) untreated (ExM), ii) 10 nM E2, or iii) 10 nM E2 + 1 μM P4 + 1 μM cAMP. After 96 h, the organoids were collected for downstream applications.

For differentiation of organoids using human pregnancy hormones, 20 ng/mL Prolactin (PRL, Peprotech 100-07), 1 μg/ml human Chorionic gonadotropin (hCG, Source Bioscience ABC403) and 20 ng/mL human placental lactogen (hPL, R&D 5757-PL) were used. Organoids were passaged routinely and after 4 d in ExM, the medium was switched to Differentiation medium (DM) which is ExM containing 10 nM E2 + 1 μM P4 + 10^{-6} M cAMP. DM was added with a combination of HCG, hPL and/or PRL for another 8 d. See Supplementary Table 3 for further information.

ELISA

Organoids from nine wells of a 48-well plate were pooled and transferred onto three 35mm ibidi μ-dishes (Thermo Scientific, 81156) thinly-coated with Matrigel diluted 1:2 in DMEM/

F12. Matrigel was removed with Matrigel cell recovery solution on ice for 1 h. Organoids were washed in DMEM/F12 and resuspended in 1.2 mL ExM. 400 µL organoid suspension was plated into each dish and incubated at 37°C for 2 h to allow organoids to attach. Dishes were flooded with ExM and cultured for 2-4 d until complete monolayers of cells had grown out. Cells were then treated as described above for E2 and P4 stimulation. Supernates were harvested after a further 96 h and centrifuged to remove any cellular material prior to concentrating to 250 µL with Vivaspin 2 concentrators (Generon, VS0291). Concentrated supernates were stored at -80°C until use. Human Osteopontin (SPP1) Platinum ELISA (eBioscience, BMS2066) was performed using 50 µL concentrated supernate with 50 µL sample buffer in duplicate alongside double diluted human SPP1 standard as per the manufacturer's instructions. Concentration of SPP1 in the supernates was calculated from the line formula of the standard plots using Microsoft Office Excel.

Immunohistochemistry (IHC)

Tissue sections of 4 µm were cut from formalin-fixed paraffin wax-embedded human endometrial and decidual tissues and organoids. Prior to paraffin embedding, organoids were removed from Matrigel using Cell Recovery Solution, fixed in formalin (Sigma, F5554) and embedded into 1% agarose (Melford, MB1200). Sections were dewaxed with Histoclear (National Diagnostics, HS-200), cleared in 100% ethanol and rehydrated through gradients of ethanol to PBS. Heat induced epitope retrieval (HIER) was performed in Access Revelation (AR) pH 6.4 buffer (A.Menarini, MP-607-PG1) or Access Super (AS) (A.Menarini, MP-606-PG1), at 125°C in an Antigen Access pressure cooker unit (A.Menarini, MP-2008-CE). Sections were blocked with 2% serum (of species in which the secondary antibody was made) in PBS, primary antibody incubation was 30 min RT°C or overnight at 4°C and slides washed in PBS. Biotinylated horse anti-mouse or goat anti-rabbit secondary antibody was used, followed by Vectastain ABC-HRP reagent (Vector, PK-6100) and developed with di-aminobenzidine (DAB) substrate (Sigma, D4168). Sections were counterstained with Carazzi's haematoxylin and mounted in glycerol/gelatin mounting medium (Sigma, GG1-10). Primary antibody was replaced with equivalent concentration of mouse or rabbit IgG for negative controls. See Supplementary Table 4 for antibody information. Periodic Acid Schiff (PAS) staining was performed on paraffin sections following standard protocols provided by Surgipath. Tissue sections were imaged using Zeiss Axiovert Z1 microscope and Axiovision imaging software SE64 V4.8.

Immunofluorescence (IF) and confocal microscopy

Endometrial organoids were grown in 35mm ibidi µ-dishes (Thermo Scientific, 81156). Organoids were incubated for 2 h at 37°C in 10 µM EdU in ExM. Organoids were fixed in 4% PFA for 30 min at RT°C and washed several times in PBS. Cells were permeabilized for 30 min in 0.5% Triton/PBS. EdU staining was done using Click-iT® EdU Alexa Fluor® 594 Imaging Kit (Thermo Scientific, C10339) following manufacturer's instructions. Organoids were washed in PBS and blocked in 5% GS/1%BSA in PBS for 40 min at RT°C. Primary antibodies were incubated in blocking buffer with 0.05% Triton at 4°C overnight. For antibodies used, see Supplementary Table 4. Negative controls were prepared by omitting primary antibody and/or omitting EdU incubation. Organoids were washed 3 times for 15 min in PBS. Organoids were incubated for 3 h RT°C in PBS with secondary antibodies (all

from ThermoFisher Scientific): AlexaFluor 488 goat anti-mouse IgG1 (A21121), AlexaFluor goat-anti-rabbit 568 (A11011) or Alexa Fluor 647 (A21244) at 1:400 and Dapi (Sigma, D9542). Organoids were washed in PBS for 30 min 3 times, mounted in ibidi mounting medium (ThermoFisher Scientific, 400241) and imaged using the ZEISS 700 Confocal microscope and ZEN Microscope Software.

Flow cytometry

Organoids were processed as described above in Organoid formation efficiency assays to obtain single cell suspension. Cells were blocked in 1% FBS in DPBS without Calcium and Magnesium (ThermoFisher Scientific, 14190136) with human IgG (Sigma, I4506) and then incubated at 4°C with SSEA-1-PE at 1:10 (Miltenyi, 130-104-936). 7-AAD was used for live/dead discrimination. Cells were sorted using a DakoCytomation MoFlo cytometer and Summit software.

In Situ Hybridization (ISH) Assays

ISH for *LRIG1* and *AXIN2* were performed on 4 μm thick paraffin sections using RNAscope 2.0 High definition assay (Advanced Cell Diagnostics) following the manufacturer's instructions. Briefly, the tissue sections were baked at 60 °C for 1 h and dewaxed with xylene, cleared in 100% ethanol and airdried. For tissue sections, the slides were treated according to the standard protocol: 10 min in Pretreat buffer 1, 15 min in Pretreat buffer 2 and 30 min at 37°C in Pretreat buffer 3. For organoid sections, milder treatments were necessary to avoid non-specific signal: Pretreat 2 for 5 min and Pretreat 3 for 15 min. Sections were then incubated with *LRIG1* probe (Cat. no. 407421) or *AXIN2* (Cat. no. 400241), positive control probe *PPIB* (Cat. no. 313901), negative control probe *dapB* (Cat no. 310043) for 2 h at 40°C. Positive and negative controls were performed for each sample. For the visualization of signal, the samples were incubated using the amplification kit and then treated with DAB for 10 min. Sections were then dehydrated, mounted in DPX (Sigma, 44581) and imaged using Zeiss Axiovert Z1 microscope and Axiovision imaging software SE64 V4.8.

Election microscopy (EM)

For Figure 1 j, k organoids were fixed in 4% glutaraldehyde in 0.1 M HEPES buffer (pH 7.4) for 12 h at 4°C, rinsed in 0.1 M HEPES buffer X5, treated with 1% osmium ferricyanide at RT°C for 12 h, followed by 5 washes in DIW. They were then treated with 2% uranyl acetate in 0.05 M maleate buffer (pH 5.5) for 12 h at RT°C, rinsed in DIW and dehydrated in an ascending series of ethanol solutions from 70% to 100% treated twice with dry acetonitrile and infiltrated with Quetol epoxy resin. Images were taken in an FEI Tecnai G2 operated at 120Kv using an AMT XR60B digital camera running Deben software. For Figure 5d, organoids were fixed in 0.5% glutaraldehyde in 0.2 M sodium cacodylate buffer (pH 7.2) for 30 min, washed in sodium cacodylate buffer, treatment with reduced osmium tetroxide 1% OsO4, 1.5% potassium ferricynide at RT°C for 60 min, washed in water, treated with 0.5% magnesium uranyl acetate at 4°C for 16 h, dehydrated with ethanol rinsed in propylene oxide and embedded in Epon resin. Ultrathin sections were examined in an FEI Tecnai G2 TEM at 80Kv. Images were acquired with MegaView III CCD and Soft Imaging Systems program.

Western blotting analysis

Organoids were incubated in Matrigel cell recovery solution on ice for 1 h to remove Matrigel, washed in ice-cold PBS and resuspended in ice cold buffer containing 20 mM Tris (pH 7.5), 150 mM NaCl, 1 mM EDTA, 1 mM EGTA, 1% Triton X-100, 2.5 mM sodium pyrophosphate, 1 mM glycerolphosphate, 1 mM Na3VO4 and complete mini proteases inhibitor cocktail (Roche, 04693159001). Western blots were performed as previously described58. Equivalent amounts of protein were resolved by SDS-PAGE, transferred onto nitrocellulose membranes. Membranes were blocked in 5% milk in TBST for 1 h at RT°C and then incubated overnight at 4°C with anti-PAEP antibody (Abcam, ab53289) diluted in 5% milk/TBST at 1:1000. The membranes were analyzed by enhanced chemiluminescence (GE Healthcare, RPN2106) using Kodak X-OMAT film (Sigma, F1274).

DNA extraction and quantification

DNA was extracted from donor patients' blood, endometrial biopsies and organoids using QIAamp DNA blood Mini kit (Qiagen). DNA was extracted from endometrial biopsies and decidual tissue by digestion with ATL buffer (Qiagen, 19076) and Proteinase K (Sigma, P4850), followed by purification steps with RNase A (Sigma, R6513) and Protein Precipitation Solution (Qiagen, 158910), precipitation with isopropanol and washing with 70% ethanol. DNA quality and concentration were determined using the Nanodrop ND-1000 Spectrophotometer.

Genetic analysis

The DNA was analysed using Agilent Sureprint G3 unrestricted CGH ISCA 8x60K array (Agilent, G4450A) by the Medical Genetics Laboratory at Cambridge University Hospital. 5 independent organoid samples were analysed and DNA from patient's blood, biopsied tissue or early passage organoids were used as hybridization controls. DNA was diluted to 50 ng/uL and labelled using the Agilent kit following manufacturer's instructions. Data analysis for segmentation and copy number calls was performed at a genome-wide resolution of 500kb using the default analysis method – CGH v2 from the Agilent CytoGenomics software Edition 2.5.8.11 (Build 37).

RNA extraction, quantification and cDNA synthesis

Total RNA was extracted using the RNeasy Mini kit with on column DNAse treatment (Qiagen, 79254), following manufacturer's instructions. RNA quality and concentration were determined using the Nanodrop ND-1000 Spectrophotometer. 500 ng-1 μg of total RNA was reverse transcribed using Superscript VILO Reverse Transcriptase (Thermo Fisher Scientific, 11754050) with random hexamers and RNAse inhibitor according to manufacturer's instructions. An RNA sample without Reverse transcriptase was used as control for genomic DNA contamination. All qRT-PCR experiments were performed with non-template control.

Real-Time PCR

Quantitative real-time PCR (qRT-PCR) was performed on 7900HT Fast Real-Time PCR system (Applied Biosystems) using Fast Taqman Mix and Taqman gene expression assays

and following manufacturer's protocol. The cycling conditions are: 95°C 20 s and 40 cycles of 95°C 3 s followed by 60°C 30 s. TaqMan Gene expression assays (Applied Biosystems) used: LIF (Hs01055668_m1), PAEP (Hs01046125_m1), SPP1 (Hs00959010_m1) and HSD17B2 (Hs00157993_m1). Expression levels were calculated applying the comparative Cycle threshold (Ct) method. Relative expression levels were normalised to the geometric mean of three housekeeping genes HPRT1 (Hs02800695_m1), TOP1 (Hs002432257_m1) and TBP (Hs00427620_m1) using Microsoft Office Excel.

Microarray expression profiling and data analysis

Microarray experiments were performed using the HumanHT-12 v4 Expression BeadChip (Illumina, BD-103-0204) according to manufacturer's instructions by the Cambridge Genomic Services at University of Cambridge. A total of 7 endometrial samples were analysed and for each, the starting glandular digest, stromal cells and established organoids were used for analysis. 6 organoid cultures derived from decidua were also analysed. RNA samples for microarray analysis were assessed for concentration and quality using a SpectroStar and a Bioanalyser. Briefly, 200 ng of Total RNA underwent linear amplification using the Illumina TotalPrep RNA Amplification Kit (ThermoFisher Scientific, AMIL1791) following manufacturer's instructions. The concentration, purity and integrity of cRNA were measured by SpectroStar and Bioanalyser. cRNA was hybridised to the HumanHT-12 v4 BeadChip overnight followed by washing, staining and scanning using the Illumina Bead Array Reader. After scanning, the data was loaded into GenomeStudio software. No background correction or normalisation is applied at this stage. The data is processed in R using the lumi package and the limma package. Across all samples probes for which the intensity values were not significantly different ($p>0.01$) from the negative controls were removed from the analysis. Following filtering the data was transformed using the Variance Stabilization Transformation (VST) from lumi and then normalised to remove technical variation between arrays using quantile normalisation. Comparisons were performed using the limma package with results corrected for multiple testing using False Discovery Rate (FDR) testing. Finally the quality of the data was assessed and the correlation of the samples in the groups compared. Heatmaps were generated using the heatmap.2 function of the R package 'gplots', which uses euclidean method to obtain the distance matrix and complete agglomeration method for clustering. For the sample heatmaps, the input is a correlation matrix based on samples' expression profile. For the gene heatmaps, the input is the vst transformed and normalized intensity matrix. The cluster analysis for the hormone stimulation microarray was done using the R sva package, expression values from all genes were transformed by removing the baseline differences between samples due to patient origin. Then, cluster analysis was done on a selected group of genes (those differentially expressed between control groups (ExM) and stimulated with Estrogen (ExM+E2) with adjusted P values ≤ 0.05) using the R stats package. The distance matrix was computed using 1-correlation as the distance measure, and hierarchical clustering was performed using the complete linkage method.

Statistics and Reproducibility

All experiments reported in this study have been reproduced with similar results using independent samples (tissues and organoids) from multiple patients. The origin of derivation

of organoids (proliferative or secretory endometrium, decidua, post-menopausal or carcinoma) and number of times the experiments were repeated are reported in figure legends and summarized in Supplementary Table 1. Given the descriptive nature of the work and biological variation between human samples, the experimental data points for each patient sample are shown separately unless stated otherwise. Statistical analyses used to analyse microarray data are reported in Methods above and in figure legends.

Supplementary Material

Refer to Web version on PubMed Central for supplementary material.

Acknowledgements

The authors are grateful to patients for donating tissue for research. We thank D. Moore, R. Remadevi, M. Baumgarten, M. Jimenez-Linan, Department of Obstetrics and Gynaecology and NHS Tissue Bank Staff at Addenbrookes University Hospital of Cambridge; H. Skelton for her invaluable histological services and technical advice; I. Pshenichnaya, Kate Bird and Andrea Starling at Stem Cell Institute for their histological services; J. Bauer and Cambridge Genomic Services for microarray analysis; I. Simonic at Medical Genetics Laboratory, Cambridge University Hospital for CGH analysis; J.N. Skepper for electron microscopic analysis; N. Miller for flow cytometry sorting; H.W. Yung and A. Sharkey for technical help and advice; J. Cross and Y.W. Loke provided much helpful discussion and all members of the Moffett lab were supportive throughout. This work was supported by Medical Research Council (MR/L020041/1), Centre for Trophoblast Research, University of Cambridge and Wellcome Trust (RG60992). M.Y.T. has received funding from E.U. 7th Framework Programme for research, technological development and demonstration under grant agreement no PIEF-GA-2013-629785. J.H. was supported by Wellcome Trust vacation scholarship. B-K. Koo is supported by a Sir Henry Dale Fellowship from the Wellcome Trust and the Royal Society (101241/Z/13/Z) and receives core support grant from the Wellcome Trust and MRC to the WT-MRC Cambridge Stem Cell Institute.

References

1. Burton GJ, Watson AL, Hempstock J, Skepper JN, Jauniaux E. Uterine glands provide histiotrophic nutrition for the human fetus during the first trimester of pregnancy. The Journal of clinical endocrinology and metabolism. 2002; 87:2954–2959. [PubMed: 12050279]
2. Hempstock J, Cindrova-Davies T, Jauniaux E, Burton GJ. Endometrial glands as a source of nutrients, growth factors and cytokines during the first trimester of human pregnancy: a morphological and immunohistochemical study. Reproductive biology and endocrinology : RB&E. 2004; 2:58. [PubMed: 15265238]
3. Gray CA, Burghardt RC, Johnson GA, Bazer FW, Spencer TE. Evidence that absence of endometrial gland secretions in uterine gland knockout ewes compromises conceptus survival and elongation. Reproduction. 2002; 124:289–300. [PubMed: 12141942]
4. Filant J, Spencer TE. Endometrial glands are essential for blastocyst implantation and decidualization in the mouse uterus. Biology of reproduction. 2013; 88:93. [PubMed: 23407384]
5. Zhang S, et al. Physiological and molecular determinants of embryo implantation. Molecular aspects of medicine. 2013; 34:939–980. [PubMed: 23290997]
6. Burton GJ, Jauniaux E, Charnock-Jones DS. Human early placental development: potential roles of the endometrial glands. Placenta. 2007; 28(Suppl A):S64–69. [PubMed: 17349689]
7. Gargett CE, Schwab KE, Deane JA. Endometrial stem/progenitor cells: the first 10 years. Human reproduction update. 2016; 22:137–163. [PubMed: 26552890]
8. Kaitu'u-Lino TJ, Ye L, Gargett CE. Reepithelialization of the uterine surface arises from endometrial glands: evidence from a functional mouse model of breakdown and repair. Endocrinology. 2010; 151:3386–3395. [PubMed: 20444944]
9. Padykula HA, et al. The basalis of the primate endometrium: a bifunctional germinal compartment. Biology of reproduction. 1989; 40:681–690. [PubMed: 2758097]

10. Ferenczy A. Studies on the cytodynamics of human endometrial regeneration. I. Scanning electron microscopy. American journal of obstetrics and gynecology. 1976; 124:64–74. [PubMed: 1244749]
11. Valentijn AJ, et al. SSEA-1 isolates human endometrial basal glandular epithelial cells: phenotypic and functional characterization and implications in the pathogenesis of endometriosis. Human reproduction. 2013; 28:2695–2708. [PubMed: 23847113]
12. Chan RW, Schwab KE, Gargett CE. Clonogenicity of human endometrial epithelial and stromal cells. Biology of reproduction. 2004; 70:1738–1750. [PubMed: 14766732]
13. Bentin-Ley U, et al. Isolation and culture of human endometrial cells in a three-dimensional culture system. Journal of reproduction and fertility. 1994; 101:327–332. [PubMed: 7932366]
14. Blauer M, Heinonen PK, Martikainen PM, Tomas E, Ylikomi T. A novel organotypic culture model for normal human endometrium: regulation of epithelial cell proliferation by estradiol and medroxyprogesterone acetate. Human reproduction. 2005; 20:864–871. [PubMed: 15665014]
15. Shahbazi MN, et al. Self-organization of the human embryo in the absence of maternal tissues. Nature cell biology. 2016; 18:700–708. [PubMed: 27144686]
16. Deglincerti A, et al. Self-organization of the in vitro attached human embryo. Nature. 2016; 533:251–254. [PubMed: 27144363]
17. Huch M, et al. Long-term culture of genome-stable bipotent stem cells from adult human liver. Cell. 2015; 160:299–312. [PubMed: 25533785]
18. Sato T, et al. Long-term expansion of epithelial organoids from human colon, adenoma, adenocarcinoma, and Barrett's epithelium. Gastroenterology. 2011; 141:1762–1772. [PubMed: 21889923]
19. Huch M, et al. Unlimited in vitro expansion of adult bi-potent pancreas progenitors through the Lgr5/R-spondin axis. The EMBO journal. 2013; 32:2708–2721. [PubMed: 24045232]
20. Karthaus WR, et al. Identification of multipotent luminal progenitor cells in human prostate organoid cultures. Cell. 2014; 159:163–175. [PubMed: 25201529]
21. Kessler M, et al. The Notch and Wnt pathways regulate stemness and differentiation in human fallopian tube organoids. Nature communications. 2015; 6:8989.
22. Chen C, Spencer TE, Bazer FW. Fibroblast growth factor-10: a stromal mediator of epithelial function in the ovine uterus. Biology of reproduction. 2000; 63:959–966. [PubMed: 10952944]
23. Sugawara J, Fukaya T, Murakami T, Yoshida H, Yajima A. Increased secretion of hepatocyte growth factor by eutopic endometrial stromal cells in women with endometriosis. Fertility and sterility. 1997; 68:468–472. [PubMed: 9314916]
24. Chung D, Gao F, Jegga AG, Das SK. Estrogen mediated epithelial proliferation in the uterus is directed by stromal Fgf10 and Bmp8a. Molecular and cellular endocrinology. 2015; 400:48–60. [PubMed: 25451979]
25. Barnea ER, Kirk D, Paidas MJ. Preimplantation factor (PIF) promoting role in embryo implantation: increases endometrial integrin-alpha2beta3, amphiregulin and epiregulin while reducing betacellulin expression via MAPK in decidua. Reproductive biology and endocrinology : RB&E. 2012; 10:50. [PubMed: 22788113]
26. Bartfeld S, et al. In vitro expansion of human gastric epithelial stem cells and their responses to bacterial infection. Gastroenterology. 2015; 148:126–136 e126. [PubMed: 25307862]
27. Bartosch C, Lopes JM, Beires J, Sousa M. Human endometrium ultrastructure during the implantation window: a new perspective of the epithelium cell types. Reproductive sciences. 2011; 18:525–539. [PubMed: 21421901]
28. Jeong JW, et al. Foxa2 is essential for mouse endometrial gland development and fertility. Biology of reproduction. 2010; 83:396–403. [PubMed: 20484741]
29. Sun X, et al. Kruppel-like factor 5 (KLF5) is critical for conferring uterine receptivity to implantation. Proceedings of the National Academy of Sciences of the United States of America. 2012; 109:1145–1150. [PubMed: 22233806]
30. Guimaraes-Young A, Neff T, Dupuy AJ, Goodheart MJ. Conditional deletion of Sox17 reveals complex effects on uterine adenogenesis and function. Developmental biology. 2016
31. Hirate Y, et al. Mouse Sox17 haploinsufficiency leads to female subfertility due to impaired implantation. Scientific reports. 2016; 6:24171. [PubMed: 27053385]

32. Wong VW, et al. Lrig1 controls intestinal stem-cell homeostasis by negative regulation of ErbB signalling. Nature cell biology. 2012; 14:401–408. [PubMed: 22388892]
33. Lim X, et al. Interfollicular epidermal stem cells self-renew via autocrine Wnt signaling. Science. 2013; 342:1226–1230. [PubMed: 24311688]
34. Gargett CE, Schwab KE, Zillwood RM, Nguyen HP, Wu D. Isolation and culture of epithelial progenitors and mesenchymal stem cells from human endometrium. Biology of reproduction. 2009; 80:1136–1145. [PubMed: 19228591]
35. Parra-Herran CE, Yuan L, Nucci MR, Quade BJ. Targeted development of specific biomarkers of endometrial stromal cell differentiation using bioinformatics: the IFITM1 model. Modern pathology : an official journal of the United States and Canadian Academy of Pathology, Inc. 2014; 27:569–579.
36. Critchley HO, Bailey DA, Au CL, Affandi B, Rogers PA. Immunohistochemical sex steroid receptor distribution in endometrium from long-term subdermal levonorgestrel users and during the normal menstrual cycle. Human reproduction. 1993; 8:1632–1639. [PubMed: 8300819]
37. Snijders MP, et al. Immunocytochemical analysis of oestrogen receptors and progesterone receptors in the human uterus throughout the menstrual cycle and after the menopause. Journal of reproduction and fertility. 1992; 94:363–371. [PubMed: 1593539]
38. Lessey BA, et al. Immunohistochemical analysis of human uterine estrogen and progesterone receptors throughout the menstrual cycle. The Journal of clinical endocrinology and metabolism. 1988; 67:334–340. [PubMed: 2455728]
39. Yang S, et al. Stromal PRs mediate induction of 17beta-hydroxysteroid dehydrogenase type 2 expression in human endometrial epithelium: a paracrine mechanism for inactivation of E2. Molecular endocrinology. 2001; 15:2093–2105. [PubMed: 11731611]
40. Maentausta O, et al. Immunohistochemical localization of 17 beta-hydroxysteroid dehydrogenase in the human endometrium during the menstrual cycle. Laboratory investigation; a journal of technical methods and pathology. 1991; 65:582–587. [PubMed: 1721669]
41. Bell SC. Secretory endometrial/decidual proteins and their function in early pregnancy. Journal of reproduction and fertility. Supplement. 1988; 36:109–125. [PubMed: 3057194]
42. Seppala M, et al. Structural studies, localization in tissue and clinical aspects of human endometrial proteins. Journal of reproduction and fertility. Supplement. 1988; 36:127–141. [PubMed: 3057195]
43. Brar AK, Frank GR, Kessler CA, Cedars MI, Handwerger S. Progesterone-dependent decidualization of the human endometrium is mediated by cAMP. Endocrine. 1997; 6:301–307. [PubMed: 9368687]
44. van der Flier LG, Haegebarth A, Stange DE, van de Wetering M, Clevers H. OLFM4 is a robust marker for stem cells in human intestine and marks a subset of colorectal cancer cells. Gastroenterology. 2009; 137:15–17. [PubMed: 19450592]
45. Spencer TE. Biological roles of uterine glands in pregnancy. Seminars in reproductive medicine. 2014; 32:346–357. [PubMed: 24959816]
46. Stewart MD, et al. Prolactin receptor and uterine milk protein expression in the ovine endometrium during the estrous cycle and pregnancy. Biology of reproduction. 2000; 62:1779–1789. [PubMed: 10819783]
47. Yang H, Lei CX, Zhang W. Human chorionic gonadotropin (hCG) regulation of galectin-3 expression in endometrial epithelial cells and endometrial stromal cells. Acta histochemica. 2013; 115:3–7. [PubMed: 21705042]
48. Saegusa M, Hashimura M, Suzuki E, Yoshida T, Kuwata T. Transcriptional up-regulation of Sox9 by NF-kappaB in endometrial carcinoma cells, modulating cell proliferation through alteration in the p14(ARF)/p53/p21(WAF1) pathway. The American journal of pathology. 2012; 181:684–692. [PubMed: 22698986]
49. Furuyama K, et al. Continuous cell supply from a Sox9-expressing progenitor zone in adult liver, exocrine pancreas and intestine. Nature genetics. 2011; 43:34–41. [PubMed: 21113154]
50. Huch M, et al. In vitro expansion of single Lgr5+ liver stem cells induced by Wnt-driven regeneration. Nature. 2013; 494:247–250. [PubMed: 23354049]
51. Huch M, Koo BK. Modeling mouse and human development using organoid cultures. Development. 2015; 142:3113–3125. [PubMed: 26395140]

52. Gjorevski N, et al. Designer matrices for intestinal stem cell and organoid culture. Nature. 2016; 539:560–564. [PubMed: 27851739]

53. Emera D, Wagner GP. Transformation of a transposon into a derived prolactin promoter with function during human pregnancy. Proceedings of the National Academy of Sciences of the United States of America. 2012; 109:11246–11251. [PubMed: 22733751]

54. Seppala M, Bohn H, Tatarinov Y. Glycodelins. Tumour biology : the journal of the International Society for Oncodevelopmental Biology and Medicine. 1998; 19:213–220. [PubMed: 9591048]

55. Arias-Stella J. The Arias-Stella reaction: facts and fancies four decades after. Advances in anatomic pathology. 2002; 9:12–23. [PubMed: 11756756]

56. Morice P, Leary A, Creutzberg C, Abu-Rustum N, Darai E. Endometrial cancer. Lancet. 2016; 387:1094–1108. [PubMed: 26354523]

57. van de Wetering M, et al. Prospective derivation of a living organoid biobank of colorectal cancer patients. Cell. 2015; 161:933–945. [PubMed: 25957691]

58. Yung HW, Korolchuk S, Tolkovsky AM, Charnock-Jones DS, Burton GJ. Endoplasmic reticulum stress exacerbates ischemia-reperfusion-induced apoptosis through attenuation of Akt protein synthesis in human choriocarcinoma cells. FASEB journal : official publication of the Federation of American Societies for Experimental Biology. 2007; 21:872–884. [PubMed: 17167073]

59. Turco MY, Gardner L, Koo BK, Moffett A, Burton GJ. Derivation and long-term expansion of human endometrial and decidual organoids. Protoc Exch. 2017; doi: 10.1038/protex.2017.030

Europe PMC Funders Author Manuscripts

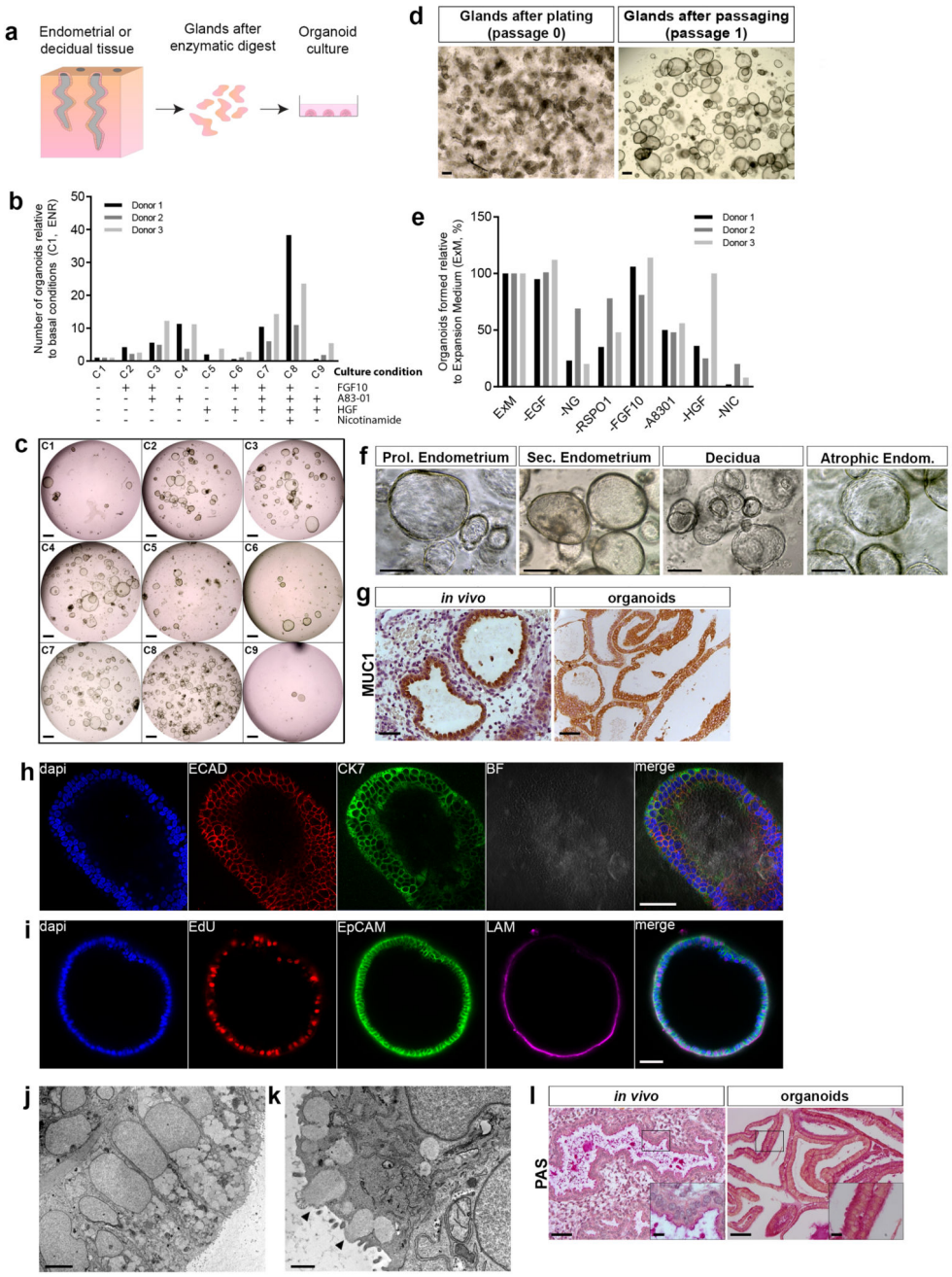

Figure 1. Long-term 3D organoid cultures can be established from human non-pregnant endometrium and decidua.

(a) Scheme for deriving organoids.

(b) Screening conditions for generating organoids. FGF10, A83-01, HGF and Nicotinamide added in combinations to generic organoid medium (ENR). Number of organoids derived under each condition (C2 to C9) shown relative to basal conditions (C1). Decidual digests from 3 different patients. Source data in Supplementary Table 5.

(c) Representative images for conditions C1-C9 in Fig. 1b. Scale bar, 500 μm.

(d) Images of decidual gland isolates (passage 0) and organoids after one passage in Expansion Medium (ExM) (passage 1). Scale bar, 200 μm. Representative of all samples, summarized in Supplementary Table 1.
(e) Effect of withdrawal of growth factors from ExM. Organoids grown in ExM and each factor withdrawn: EGF, Noggin (NG), Rspondin-1 (RSPO1), FGF10, A8301, HGF and Nicotinamide (NIC). Organoids formed shown relative to ExM (%). Shown are decidual cultures derived from 3 different patients. Source data in Supplementary Table 5.
(f) Images of organoids established in ExM from proliferative (Prol.) endometrium (n=3), secretory (Sec.) endometrium (n=9), decidua (n=25) and post-menopausal (atrophic) endometrium (n=1). Scale bar, 100 μm.
(g) IHC of decidua (*in vivo*) and organoids for Mucin 1 (MUC-1). Scale bar, 50 μm. Representative of 6 decidual and endometrial samples, and organoids derived from 2 endometrial and 2 decidual samples from different patients.
(h) IF staining of organoid for E-CADHERIN (E-CAD) and CYTOKERATIN-7 (CK7). Scale bar, 50 μm. Experiment repeated twice (1 endometrial-derived and 1 decidua-derived organoids).
(i) IF staining of organoid for cell proliferation (uptake of EdU), epithelial marker EPCAM and basement membrane marker laminin (LAM). Scale bar, 50 μm. Experiment repeated twice (1 endometrial-derived and 1 decidua-derived organoids).
(j) Electron micrograph (EM) of organoid showing columnar epithelial cells with basally-located nuclei. Scale bar, 5 μm. Experiment repeated twice with different donors.
(k) EM showing secretory activity (black arrowheads). Scale bar, 1 μm. Experiment repeated twice with different donors.
(l) PAS staining for glycogen in endometrium and organoids. Scale bars, 50 μm (main image) and 10 μm (inset). Representative of 3 endometrial samples and 3 endometrial organoids.

Europe PMC Funders Author Manuscripts

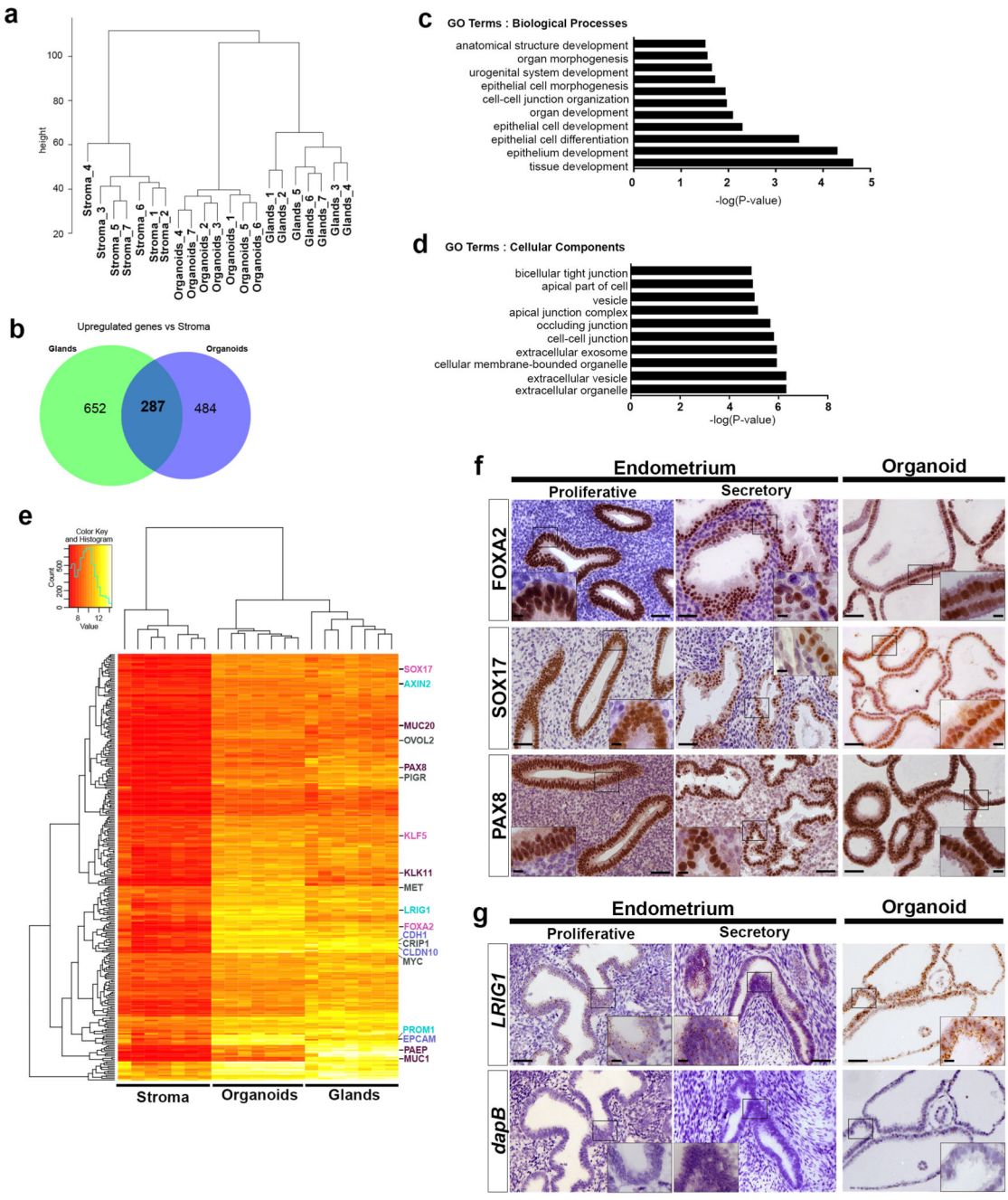

Figure 2. Established human endometrial organoids recapitulate molecular signature of glands *in vivo*.

(a) Unsupervised hierarchical clustering analysis of global gene expression profiles by microarray of gland digests, stromal cells and corresponding established organoids from endometrium (n=7 independent donors). Analysis based on 15475 probes with sd/mean >0.1. Expression profiles of organoids cluster with glands while those of the stroma cluster in a separate tree.

(b) Venn diagram showing overlap of 287 genes significantly upregulated in glands and organoids with a fold change ≥1.5 (p≤0.01) relative to stroma.

Europe PMC Funders Author Manuscripts

(c) Gene ontology (GO) analysis of the 287 genes from (b) using HumanMine v2.2 database for GO Terms Biological processes and Benjamini Hochberg test correction with maximum p-value of 0.05. The top ten significantly enriched GO terms for each category are shown with the –log of their p-values and are enriched for terms describing epithelial tissue.
(d) Gene ontology (GO) analysis of the 287 genes from (b) using same method as in (c). The top ten significantly enriched GO terms describe epithelial cells with secretory function.
(e) Clustered heatmap of 287 genes commonly upregulated between organoids and glands compared to stroma from (b). Genes of interest are listed on the right. Epithelial markers (blue) (*EPCAM, CLD10, CDH1*), glandular products and markers of secretory cells (purple) (*MUC20, PAX8, PAEP, MUC1*), progenitor cell markers (cyan) (*LRIG1, PROM1, AXIN2*) and murine genes important for endometrial function (pink) (*SOX17, KLF5, FOXA2*).
(f) IHC for genes selected from microarray, FOXA2, SOX17 and PAX8, in proliferative and secretory endometrium and organoids. Scale bars, 50 μm (main image) and 10 μm (insets). Representative of 3 proliferative and 7 secretory endometrial samples and endometrial organoids derived from 8 different patients.
(g) ISH for *LRIG1* on proliferative and secretory endometrium and organoids. Negative control probe is for the bacterial gene *dapB*. Scale bars, 50 μm (main image) and 10 μm (insets). Representative of 3 proliferative and 3 secretory endometrial samples and endometrial organoids derived from 4 different patients.

Europe PMC Funders Author Manuscripts

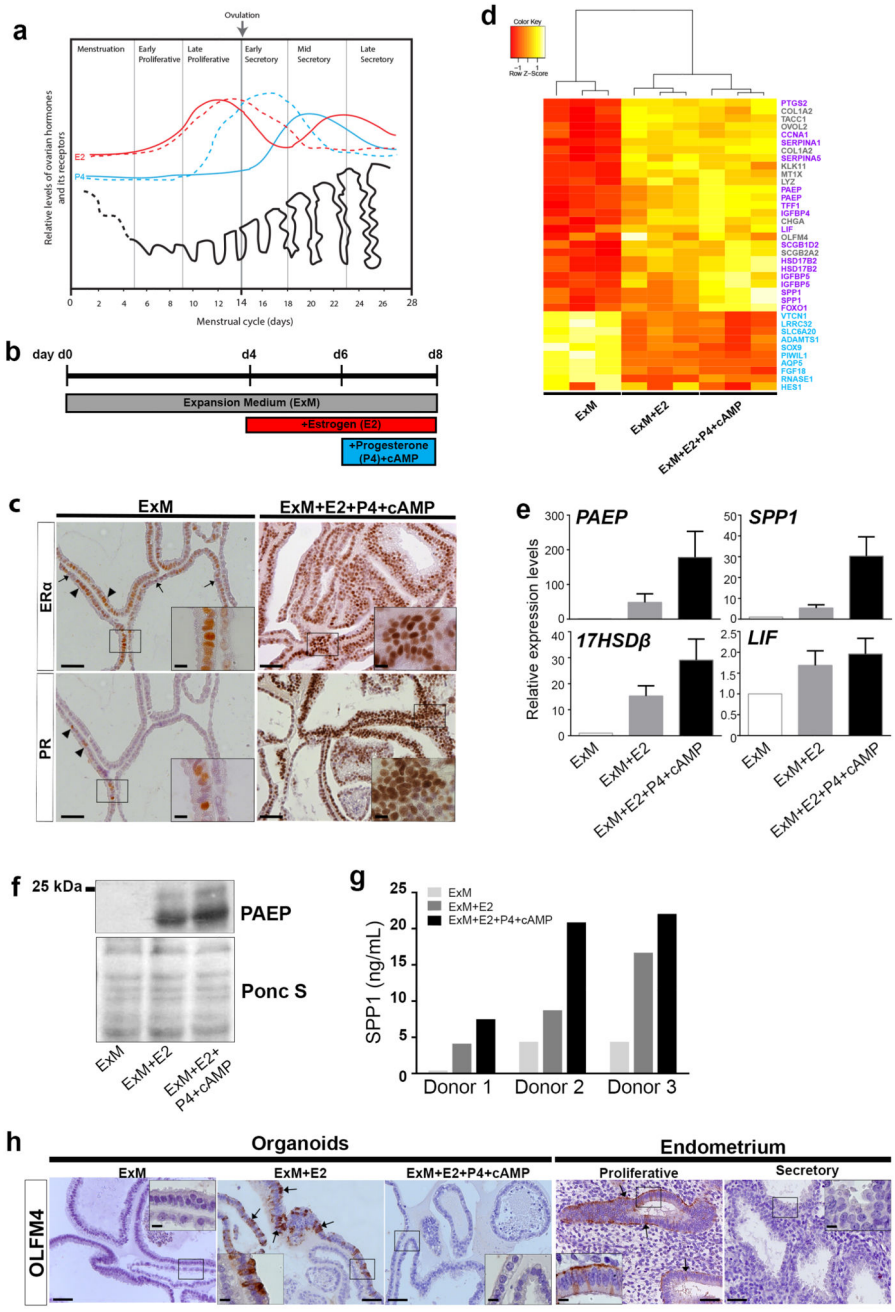

Figure 3. Human endometrial organoids respond to sex hormones.

(a) Ovarian hormones, Estrogen (E2)(red), Progesterone (P4)(blue), and the cycling endometrium. Expression of Estrogen Receptor (ERα)(dashed red) and Progesterone Receptor (PR)(dashed blue) are specific for glands of the functional layer. Adapted from Reference37.

(b) Hormonal stimulation. Organoids grown in ExM, day 0 (d0), are primed with E2 for 48 h on day 4 (d4) followed by stimulation with P4 and cyclic AMP (cAMP) for 48 h.

(c) IHC for ERα and PR on organoids after hormonal stimulation. In ExM expression of ERα is weak, but some cells are either ERα^{high} (arrowheads) or ERα^{negative} (arrows). Few cells are positive for PR (arrowheads). After E2 and P4 treatment, levels of ERα and PR are higher. Scale bars, 50 μm (main image), 10 μm (insets). Representative of endometrial organoids from 6 patients and decidual organoids from 9 patients.
(d) Clustered heatmap of selected genes from organoids grown in ExM, ExM+E2 or ExM +E2+P4+cAMP (n=3 donors). Shown are genes known to reflect differentiation in response to hormones (purple), uncharacterized genes (grey) and downregulated genes (cyan).
(e) QRT-PCR analysis for differentiation markers (*PAEP, SPP1, 17HSDβ2* and *LIF*) of organoids grown in ExM, ExM+E2 or ExM+E2+P4+cAMP. Shown is the mean±SEM levels of expression relative to housekeeping genes and ExM conditions (δδCt). Data from endometrial organoids from n=6 different patients. Source data in Supplementary Table 5.
(f) Western blot for PAEP in organoids after hormonal stimulation. Levels of glycosylated and non-glycosylated PAEP increase upon exposure to E2 and E2+P4+cAMP. Ponceau S staining (Ponc S) for loading control. Experiment repeated twice using endometrial organoids from 2 patients. Unprocessed blots in Supplementary Figure 7.
(g) ELISA for SPP1 production by endometrial organoids upon exposure to hormones. Three independent experiments (Donors 1-3). SPP1 secretion increases following exposure to E2 and further after E2+P4+cAMP. Source data in Supplementary Table 5.
(h) IHC for OLFM4 on organoids under ExM, ExM+E2 and ExM+E2+P4+cAMP, and proliferative and secretory endometrium. Scale bars, 50 μm (main image) and 10 μm (insets). Representative of 2 proliferative and 2 secretory endometrial tissues and organoids derived from 3 different patients.

Europe PMC Funders Author Manuscripts

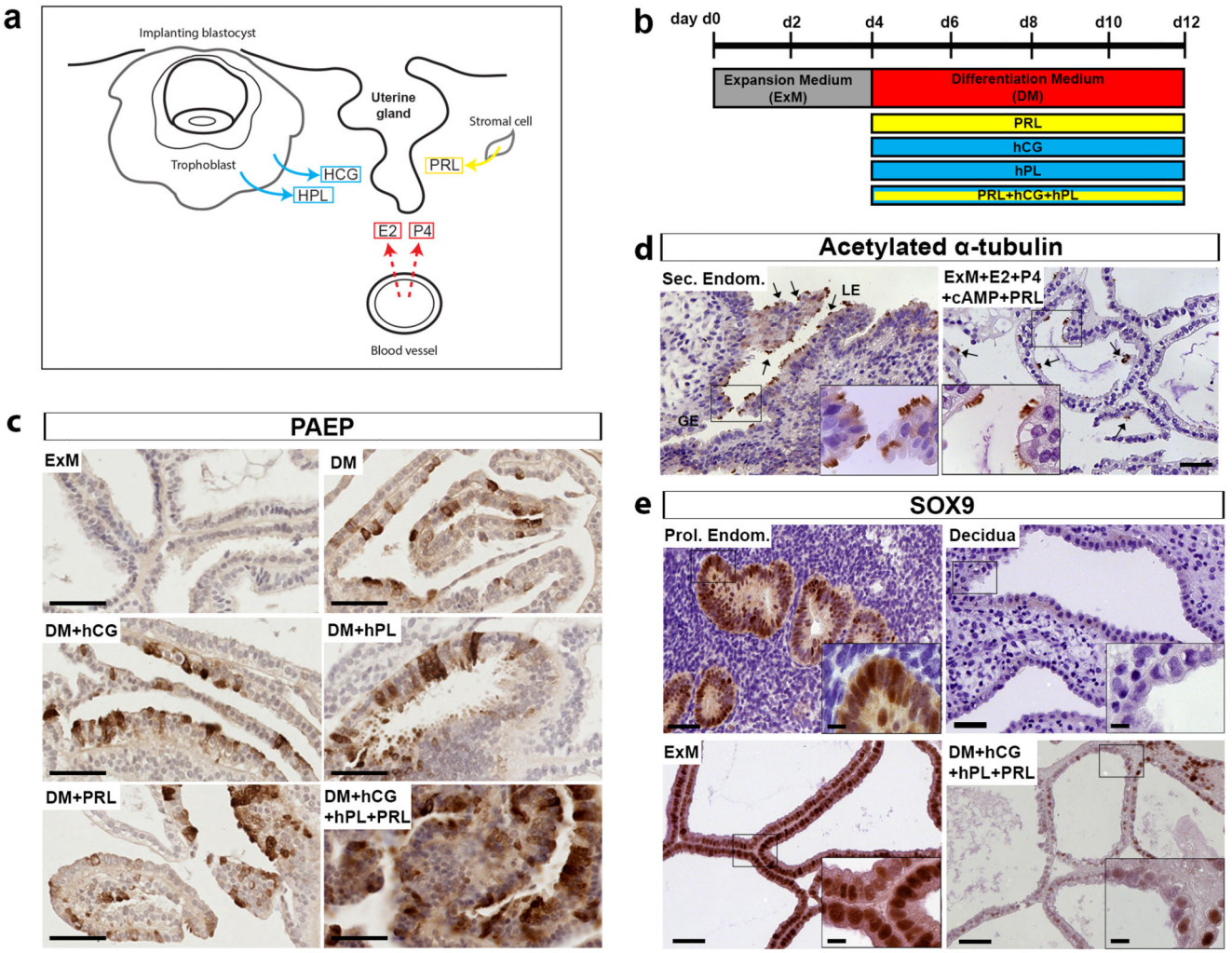

Figure 4. Signals from decidualised stroma and the placenta can further stimulate differentiation of human endometrial gland organoids.

(a) Hormonal environment of endometrium during the first trimester of pregnancy. Estrogen (E2) and Progesterone (P4) are ovarian products, human chorionic gonadotropin (hCG) and human placental lactogen (hPL) are secreted by trophoblast and prolactin (PRL) by decidualized stromal cells.

(b) Protocol for stimulation of endometrial organoids. Organoids are passaged and plated on day 0 (d0) in ExM. On d4, ExM is changed to Differentiation Medium (DM; ExM with E2+P4+cAMP). hCG, hPL and/or PRL were added for 8 d.

(c) IHC for PAEP on endometrial organoids under the following conditions: ExM, DM, DM with hCG/hPL or PRL or all three combined. Maximal production of PAEP and differentiated morphology of cells is seen upon exposure to DM with hCG, hPL and PRL. Scale bar, 50 μm. Representative of endometrial organoids derived from 3 different patients.

(d) IHC for acetylated α-tubulin to visualize cilia in secretory endometrium (Sec. Endom.) and endometrial organoids following stimulation with PRL. Ciliated cells (arrows) are present in the luminal epithelium (LE) and within organoids. GE, glandular epithelium.

Scale bars, 50 μm (main image) and 10 μm (insets). Representative of 4 secretory endometrial samples and endometrial organoids derived from 4 different patients. (e) Immunohistochemistry for SOX9 on endometrial glands (*in vivo*) and organoids. Organoids in ExM express high levels of SOX9 similar to proliferative endometrium (Prol. Endom.). After hormonal stimulation, SOX9 is downregulated in organoids (ExM+HCG +HPL+PRL) similar to glands in decidua. Scale bars, 50 μm (main image) and 10 μm (insets). Representative of 4 proliferative endometrial samples, 7 decidual samples and endometrial organoids derived from 4 different patients.

Europe PMC Funders Author Manuscripts

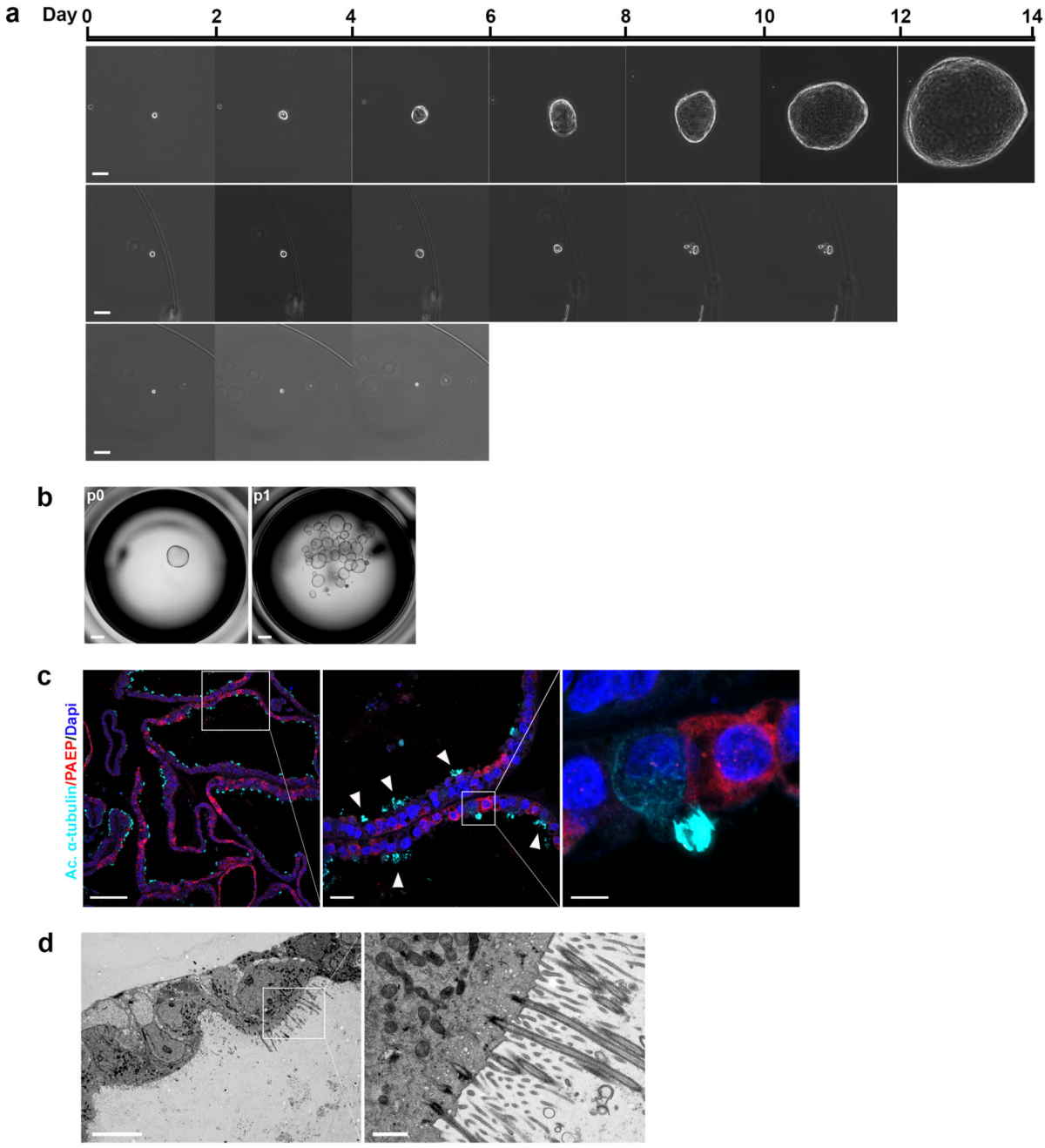

Figure 5. Human endometrial organoids have clonogenic ability and are bipotent.

(a) Phase-contrast images of (from top to bottom row): an organoid forming from a single cell; a single cell forming a spheroid with no further growth, and a single cell showing no growth. Images were taken every two days. Scale bar, 50 μm. Experiment was performed with 3 clonal lines derived from 2 endometrial and 1 decidual organoid cultures.

(b) Representative image showing expansion of a clonal culture at passage 1 (p1) from a single organoid (at passage 0, p0) in a 96-well. Scale bar, 500 μm. 12 clonal cultures were

Europe PMC Funders Author Manuscripts

established from organoids from 5 different patient samples (4 endometrial-derived and 1 decidual-derived).

(c) IF on clonally-derived endometrial organoid cultures subjected to the full cocktail of hormonal stimuli to visualize two main endometrial epithelial cell types: ciliated cells (acetylated α-tubulin) (cyan) and secretory cells (PAEP) (red). Scale bars from left to right: 100 μm, 20 μm and 5 μm. Representative of 4 clonal lines derived from 2 different endometrial organoid cultures.

(d) EM on clonally-derived endometrial organoid cultures subjected to the full cocktail of hormonal stimuli showing basal bodies of fully formed cilia. Scale bars: 10 μm and 1 μm. Experiment performed twice using 1 clonal endometrial organoid culture.

Europe PMC Funders Author Manuscripts

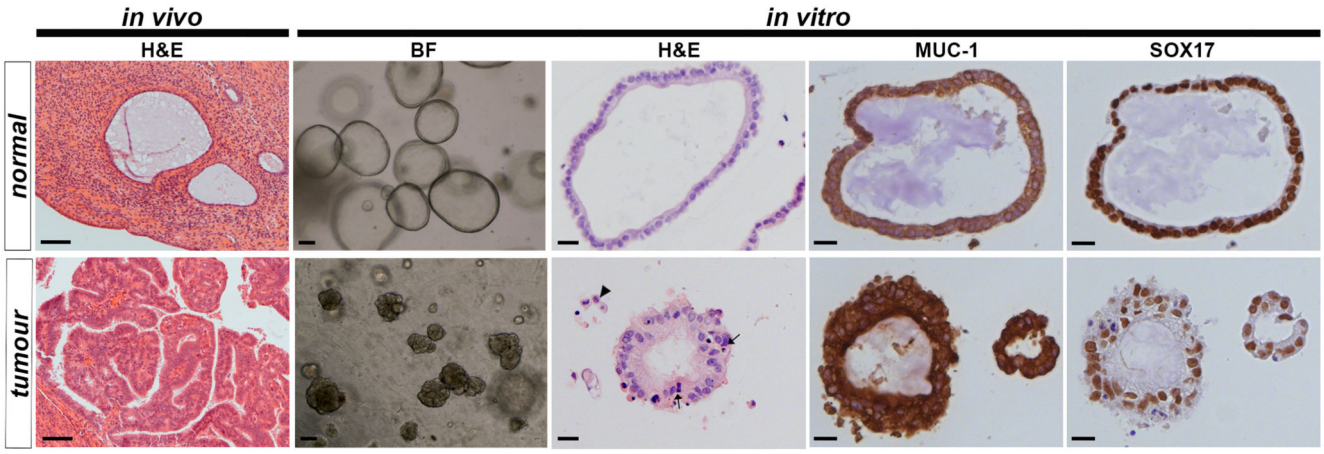

Figure 6. Organoids can be derived from endometrial cancer.

Derivation of organoids from endometrial carcinomas. From left to right: H&E stained sections of normal atrophic endometrium showing gland surrounded by dense stroma and a FIGO Grade I endometrioid carcinoma with dense glandular structures from the same patient, scale bar, 100 μm; images of organoids derived from matched normal and malignant endometrium cultured in ExM (passage 1), scale bar, 100 μm; H&E stained sections showing marked differences in morphology between organoids derived from normal endometrium and those from tumours which show nuclear pleomorphism, a disorganized epithelium with irregular basement membrane and isolated cells present in surrounding Matrigel (arrows), scale bar, 20 μm; IHC for MUC-1 and SOX17 on tumour and normal organoids confirm their glandular origin, scale bar, 20 μm. Representative of organoids derived from 3 different endometrial carcinomas and 1 matching normal tissue.

Europe PMC Funders Author Manuscripts